# MIMO Optical Wireless Communication via Monolithic or Sparse Apertures

# MIMO Optical Wireless Communication via Monolithic or Sparse Apertures

Majid Safari, Shenjie Huang

***Abstract*—In this paper, a general optical wireless communication (OWC) system impaired by atmospheric turbulence is studied. It is shown that if the geometry of the overall OWC system lies in the near-field regime, it can benefit from the advantages of a full multiple-input multiple-output (MIMO) system whether it is implemented by monolithic or sparse apertures. A unified framework is presented to analyze such MIMO OWC systems and their achievable diversity and multiplexing gains are estimated. Moreover, assuming that the size of OWC transceivers and the number of utilized degrees of freedom are constrained, the performance of MIMO OWC systems using monolithic or sparse apertures are compared. The results show that the multiplexing systems with monolithic apertures outperform those with sparse apertures in weaker turbulence conditions but it is expected that their superiority vanishes in the presence of strong turbulence. In terms of spatial diversity, the two design approaches provide similar gains.**

## I. Introduction

Optical wireless communication refers to data transmission using unguided light propagating through free space over ranges of few meters to thousands of kilometres. This technology is commonly known as free-space optical (FSO) communication in outdoor terrestrial and space applications. Such applications would be of great importance for future 5G systems by expanding the terrestrial backhaul network in urban areas [1], providing internet for remote areas by establishing high-speed space/air to ground networks [2], and quantum communication [3]. FSO systems typically employ coherent laser sources to generate highly directed beams propagating through atmosphere over a line-of-sight link. The propagation of the optical signal over the atmospheric channel is impaired by a number of effects including scattering, absorption, diffraction, and atmospheric turbulence.

The practical deployment of multiple transmitters and receivers in communication systems has opened up avenues for research on a number of innovative techniques to improve the capacity and/or the reliability of communication systems by providing power, diversity and/or multiplexing gains. MIMO multiplexing techniques can offer a larger number of spatial degrees of freedom (DoFs) through the employment of multiple transmitters/receivers, enabling transmission of several data streams in parallel. On the other hand, MIMO diversity schemes improve the reliability by reducing the probability of outage caused by random signal amplitude fluctuations which is an inherent feature of wireless channels. This can be guaranteed through spatial diversity schemes that transmit the same data stream over several independent diversity paths created by the underlying MIMO structure.

The success of MIMO techniques in enhancing the capacity and reliability of radio-frequency (RF) wireless communication systems has led to a renewed adoption of this approach in FSO systems. However, only few works have investigated the capacity enhancement capability of MIMO multiplexing techniques for FSO communication through asymptotic analysis and capacity bounds [4], [5]. On the other hand, many works have recently studied the application of MIMO diversity techniques in improving the reliability of FSO systems hampered by effects such as atmospheric turbulence [6]–[16]. Distortions caused by turbulence lead to the fluctuations of received optical intensity, an effect known as scintillation or fading which is also studied in the context of RF wireless communications. The turbulence-induced fading is slow varying and therefore causes long outages particularly in longer FSO links.

Spatial-mode multiplexing (SMM) in FSO is similar to mode-division multiplexing in optical fibers, which has recently attracted attention of many researchers [17], [18]. SMM enables FSO systems with a single monolithic aperture to transmit multiple streams of data carried by orthogonal spatial modes selected from a particular mode set such as Laguerre-Gaussian (LG) beams [19] or Hermite-Gaussian (HG) beams [20]. Similar to conventional MIMO systems that employ a sparse aperture (multiple separated apertures), SMM can achieve high spatial DoFs for communication although a single monolithic aperture is used. Most of the recent literature investigating SMM-based FSO systems has focused on orbital angular momentum (OAM) modes mainly due to their smaller space-bandwidth product and the availability of practical (de)multiplexing techniques [17], [20]. However, these modes are only a subset of the complete LG basis and may offer a lower number of spatial DoFs than the conventional MIMO [20]. While SMM generally enhances the capacity of FSO systems, its performance is impaired in the presence of strong atmospheric turbulence as the mode orthogonality can not be preserved after propagation through the atmosphere [21]. Recently, in [22], [23], the so-called spatial *mode diversity* FSO systems were proposed based on multi-mode transmission from monolithic apertures to combat the degrading effects of turbulence.

In this paper, we study the performance of FSO communication systems either implemented with sparse or monolithic apertures. We present a unified framework based on which both transceiver designs can be analyzed as MIMO systems. While the literature has been mostly focused on the diversity advantage of conventional MIMO (sparse-aperture) FSO systems and the multiplexing advantage of multi-mode (monolithic-aperture) FSO systems, we show the capability

of both designs in providing both multiplexing and diversity gains. We finally compare the performance of systems designed by monolithic or sparse apertures in terms of diversity and multiplexing gains in different turbulence conditions.

## II. Conventional MIMO FSO Communication Systems

Conventional MIMO FSO systems employ multiple sources emitting from individual apertures at the transmitter side and multiple detectors fed by individual apertures at the receiver side. Such MIMO structures can be exploited to increase the capacity of FSO systems through multiplexing when independent data streams are transmitted from the multi-aperture transmitter. In addition, MIMO FSO can enhance the reliability of FSO links degraded by atmospheric turbulence by transmission of redundant data through multiple sources. Considering the fact that the fading caused by atmospheric turbulence is slowly varying, most of the literature on conventional MIMO FSO systems has focused on diversity techniques. Spatial diversity can effectively mitigate fading effects and significantly reduce the probability of long outages that can affect millions of bits in each faded channel state.

Spatial *receive* diversity schemes are based on efficient combining of copies of the same signal received at different receive apertures using methods such as selection combing, equal gain combining and maximal ratio combining. Aperture averaging effect is an example of receive spatial diversity that is observed in FSO systems with large monolithic apertures and has been known for several decades [24]. It indicates that the direct-detection FSO receiver with a large aperture performs an inherent equal gain combining on differently distorted parts of a beam propagated through the turbulent atmosphere. However, spatial receive diversity using monolithic (aperture averaging) or sparse apertures may not be sufficient to combat fading. This is particularly important as the size of transceivers and thus the ability to employ large receive apertures are limited while optical power emitted from a single transmit aperture is also constrained by eye-safety regulations.

The spatial *transmit* diversity can also be used to improve the reliability of communication systems especially when receivers are limited in size, cost, and complexity. However, realizing efficient transmit diversity did not seem as straightforward as receive diversity and remained an open problem for many years. This is because simply sending the same signal from different transmit nodes (i.e., repetition coding) does not provide diversity gain in coherent communication systems. Therefore, space-time coding (STC) techniques proposed in RF wireless communication to address this issue and provide diversity by orthogonalizing the channels through which the multiple copies of signal are transmitted [25]. Following the success of STC in RF communications, attempts were made to adapt them to intensity modulation direct detection (IMDD) FSO systems [14], [26] which are most common in practice. In effect, new sets of codes can be designed to achieve full transmit diversity gain without requiring the knowledge of signal polarity (phase). However, in [10], it has been shown that the use of STC (e.g., orthogonal space-time block codes) is not required in IMDD FSO communication to achieve transmit diversity and it can be even detrimental in some cases while adding complexity. This is because even by simply transmitting the (uncoded) copies of the same signal from multiple apertures that are sufficiently separated, the received signal can be modelled as incoherent superposition of the transmitted copies and is not degraded by destructive interference.

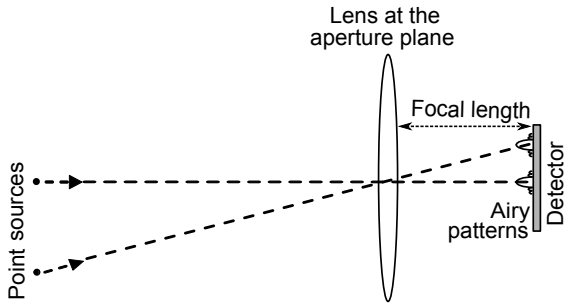


Fig. 1. The Airy pattern images of two beams emitted from distant separated sources are generated by a lens located at the aperture plane of a FSO receiver. The spatial orthogonality of the Airy patterns is demonstrated on the detector area which is positioned at the focal plane of the aperture lens. Note that the size of the detector and Airy patterns ($\mu$m range) are much smaller than the lens (cm range) but they are illustrated in comparable scale for presentation.

Figure 1 shows the receiver side of a typical FSO systems where the optical field collected at the receive aperture is focused by a lens onto the detector area located at the focal plane of the focusing lens. The diffracted field produced in the focal (detector) plane, forms so-called "Airy patterns" occupying a width in the order of optical wavelength. The Airy pattern image of two separated point sources produced by the lens on the detector plane is shown in Fig. 1. Since the optical lens performs a linear transformation (i.e., Fourier transform) of the incident optical field which is the superposition of the received optical field from individual sources, the Airy patterns are also superimposed in the focal plane. However, if the multiple transmit apertures are sufficiently separated, the corresponding received Airy patterns would be spatially orthogonal and thus the photodetector simply detects the addition of the optical power of the individual signals (i.e., incoherent addition) allowing for the realization of full transmit diversity gain through simple repetition coding [7], [8], [10].

Majority of the works focusing on the performance of MIMO FSO system have simplified their analysis by considering a common set of assumptions. For example, it is typically assumed that the transmit and receive apertures are small compared to the spatial coherence length of the turbulent atmosphere and the distance between source and destination is assumed to be much greater than the receive and transmit aperture diameters. These assumptions reduce the general description of the turbulence effect from a 2D$\times$2D random process (from transmit aperture area to receive aperture area) into a single random variable. Another simplifying assumption

commonly made for MIMO systems is that the multiple apertures are sufficiently separated at both sides such that the corresponding random variables describing the fading of individual diversity paths are statistically independent.

Diversity gain is conventionally defined as how fast the logarithm of system performance curve (e.g., outage probability or average bit error rate) decays with respect to $\log(SNR)$ at high signal-to-noise ratio (SNR). Therefore, the outage probability $P_{\text{out}}$ of the MIMO FSO diversity system with $N_t$ transmit apertures and $N_r$ receive apertures, defined based on the assumptions above, scales at high SNR as

$$P_{\text{out}} \approx e^{-N_t N_r D_S \log(SNR)}, \tag{1}$$

where $D_S$ is the diversity gain of the corresponding single-input single-output (SISO) link. Unlike RF communication where $D_S = 1$, in FSO communication, $D_S$ can deviate from unity and can even depend on SNR at weak turbulence conditions. For example, it can be shown that $D_S \approx \log(SNR)/8\sigma_\chi^2$ for weak turbulence ($\sigma_\chi^2 \ll 1$) wherein the fading is modelled by lognormal distribution [27] and $D_S = \min\{\alpha, \beta\}/2$ for medium or strong turbulence conditions when Gamma-Gamma distribution is used [14] where $\sigma_\chi^2$ is the variance of turbulence-induced log-amplitude fluctuations and $\alpha$ and $\beta$ are the parameters of the Gamma-Gamma fading model. Equation (1) shows that the relative diversity gain of the underlying MIMO FSO system with respect to a SISO system is determined by the product of the number of transmit and receive apertures, $N_t N_r$ similar to RF MIMO diversity systems. In [28], the random misalignment caused by pointing errors is analyzed as fading and it is shown that the achievable diversity gain in the presence of weak turbulence and misalignment is dominated by the ratio of the received beam size to the misalignment variance rather than the number of transmit/receive apertures. However, in strong turbulence conditions, both the received beam size and the number of transmit/receive apertures affect the achievable diversity gain [29].

Unfortunately, the common set of assumptions mentioned earlier impose limitations on the geometry of underlying MIMO FSO systems such that important effects such as aperture averaging, turbulence correlation and some other near-field effects typically observed in practical FSO systems are ignored. A number of works in the literature have focused on such effects although providing a generalized theoretical framework is cumbersome. In [30], through numerical modelling, the impact of the spatial correlation was investigated on the performance of a multi-aperture diversity FSO system and a simple scaling rule was proposed to describe spatial correlation coefficient in terms of the link length. In [15], using both numerical and analytical modelling, the near-field effects of a multi-beam FSO communication system was studied and the effect of fading correlation on achievable diversity gain was shown. Furthermore, the aperture averaging effect has been investigated in many works in the literature. For example, in [12], it has been shown that, under background-limited regime, a sparse-aperture receive diversity system outperforms the monolithic-aperture FSO system assuming that the two systems have the same effective aperture areas and that the received signals at individual subapertures of the sparse aperture are affected by statistically independent fadings.

## III. A Unified MIMO Channel Model

As discussed in the section II, conventional MIMO FSO systems designed based on sparse apertures have focused on the use of spatial diversity to enhance reliability of operation over the turbulent atmospheric channel. On the other hand, multi-mode transmission in FSO systems has been commonly used for multiplexing. In this section, we present a unified model to analyze general FSO systems either implemented with monolithic or sparse apertures as MIMO systems capable of providing both multiplexing and diversity.

### A. The Degrees of Freedom of FSO Channels

One of the most important features of any communication channel, particularly when channel capacity is concerned, is the number of degrees of freedom that it supports for parallel data transmission. The number of DoFs indicates the dimension of the signal space extended over the available (spectral, temporal, spatial etc.) resources that can be reliably detected at the receiver. Here, we are interested in the number of spatial DoFs of a FSO system to predict the potential of MIMO FSO systems.

FSO communication links provide line-of-sight (LoS) connectivity where the propagation of light can be impaired by a number of atmospheric effects. This includes absorption and scattering of the optical beam propagating through the atmosphere caused by aerosols and molecules particularly in adverse weather conditions. Furthermore, atmospheric turbulence creates random fluctuations of refractive index over the atmospheric channel distorting the spatial phase of the transmitted beam along the propagation path eventually leading to fading in the received optical signal. The aperture sizes at both sides of FSO links are typically much greater than the optical wavelength and this gives the impression that very large MIMO sizes can be realized. However, the effective number of DoFs in FSO links are practically limited by effects such as diffraction and turbulence.

In order to define a unified framework to analyze the performance of FSO systems implemented using either monolithic (e.g., multi-mode transmission systems) or sparse (e.g., conventional MIMO systems) apertures, we constrain the spatial resources of the two schemes by limiting the size of transmit/receive apertures. As shown in Fig. 2(a) and 2(b), the single monolithic aperture or multiple sub-apertures need to be confined within the defined extended circular aperture areas at both transmitter ($\mathcal{R}$) and receiver ($\mathcal{R}'$) sides. Consider an encoded light beam with spatial field pattern $\xi(\mathbf{r})$ is transmitted from the extended circular aperture $\mathcal{R}$ with coordinates $\mathbf{r}$ and radius of $R_1$. Based on the extended Huygens-Fresnel principle, the propagated field pattern $\xi'(\mathbf{r}')$ at the received aperture $\mathcal{R}'$ with radius $R_2$ located $L$ meters away from source can be expressed as

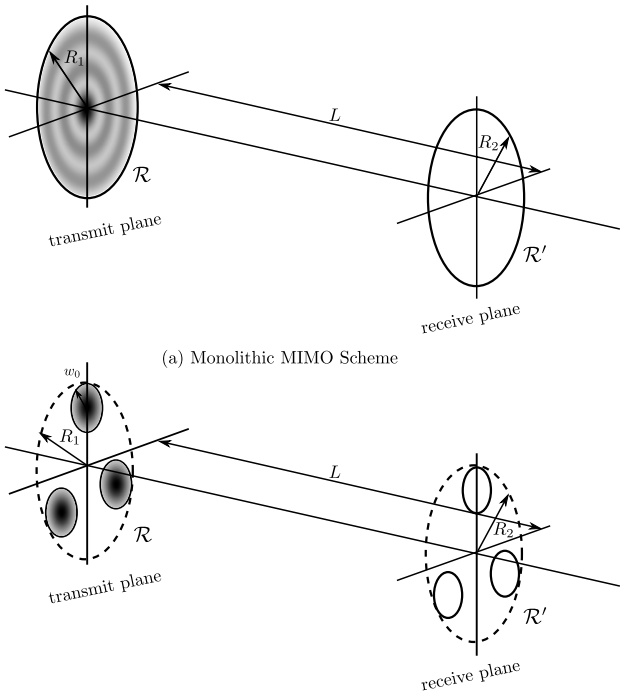


(a) Monolithic MIMO Scheme

(b) Sparse MIMO Scheme

Fig. 2. A Schematic diagram of a MIMO FSO system whether implemented based on a) monolithic or b) sparse apertures. The input beam pattern $\xi(\mathbf{r})$ can be properly defined over the transmit aperture $\mathcal{R}$ to describe either design.

$$\xi'(\mathbf{r}') = \int_{\mathcal{R}} \xi(\mathbf{r}) h(\mathbf{r}, \mathbf{r}') e^{-aL/2} d\mathbf{r}, \tag{2}$$

where $a$ determines the loss due to absorption and scattering and $h(\mathbf{r}, \mathbf{r}')$ denotes the paraxial Green's function for turbulent atmospheric propagation given by

$$h(\mathbf{r}, \mathbf{r}') = \frac{e^{jkL + jk|\mathbf{r}-\mathbf{r}'|^2/2L}}{j\lambda L} e^{\chi(\mathbf{r},\mathbf{r}') + j\varphi(\mathbf{r},\mathbf{r}')}, \tag{3}$$

where $\lambda$ is the wavelength, $k = 2\pi/\lambda$ is the wave number and $\chi(\mathbf{r}, \mathbf{r}')$ and $\varphi(\mathbf{r}, \mathbf{r}')$ are the stochastic log-amplitude and phase fluctuations respectively induced by atmospheric turbulence of the path connecting points $\mathbf{r}$ and $\mathbf{r}'$. It is important to note that by properly defining the extended apertures $\mathcal{R}$ and $\mathcal{R}'$ (e.g., using window functions for sparse aperture) and input field pattern $\xi(\mathbf{r})$, any LoS FSO transmission system either with monolithic or sparse aperture can be modelled by (2). Moreover, in order to encode/decode spatial signatures (i.e., field patterns) on the transmitted beams in Fig. 2(a), spatial light modulators and optical (de)multiplexers are required. The sparse aperture design in Fig. 2(b) can be also thought of a monolithic aperture design where simple multi-aperture masks act as optical (de)multiplexers. To obtain the number of DoFs for the general FSO channel defined above, we can take the singular value decomposition (SVD) of $h(\mathbf{r}, \mathbf{r}')$ which is given by [31]

$$h(\mathbf{r}, \mathbf{r}') = \sum_{n=1}^{\infty} \sqrt{\mu_n} \phi_n(\mathbf{r}') \Phi_n^*(\mathbf{r}), \tag{4}$$

where the eigenvalues $\mu_n \in [0, 1]$ are in descending order while $\{\Phi_n(\mathbf{r})\}$ and $\{\phi_n(\mathbf{r}')\}$ are the input and output eigenfunction vectors, respectively. In addition, $\{\Phi_n(\mathbf{r})\}$ and $\{\phi_n(\mathbf{r}')\}$ constitute complete orthonormal sets on $\mathcal{R}$ and $\mathcal{R}'$, respectively. Note that these eigenvalues and eigenfunctions are generally random because of the turbulence induced random term in the atmospheric Green's function in (3) (i.e., $e^{\chi(\mathbf{r},\mathbf{r}')+j\varphi(\mathbf{r},\mathbf{r}')}$), but their statistics are not known. Assuming that the complete channel state information (CSI) of the 2D×2D channel defined by $h(\mathbf{r}, \mathbf{r}')$ is available at both transmitter and receiver, the eigenvalues and eigenfunctions can be calculated numerically for each channel state. Then, the transmitter can use adaptive optics to shape the input beam pattern based on the instantaneous eigenfunctions of the channel and exploit DoFs of the FSO system to achieve maximum multiplexing gain through multimode transmission. An important parameter that give some insights into the DoFs of the FSO channel is the eigensum of the channel defined as [31]

$$D_f = \int_{\mathcal{R}} \int_{\mathcal{R}'} |h(\mathbf{r}, \mathbf{r}')|^2 d\mathbf{r} d\mathbf{r}' = \sum_{n=1}^{\infty} \mu_n, \tag{5}$$

which indicates whether the FSO system operates in a near field ($D_f \gg 1$) or far field ($D_f \ll 1$) regimes. In the far field, only one nonzero eigenvalue prevails and thus $\mu_1 \approx D_f$ while in the near field there exist $D_f$ eigenfunctions (spatial modes) with eigenvalues close to 1 [31]. The maximum multiplexing gain of a general FSO system at each channel state can be described by the available DoFs of the channel and is thus given by

$$M_{\max} = N_{\text{DoF}} \approx \begin{cases} D_f, & \text{Near field,} \\ 1, & \text{Far field.} \end{cases} \tag{6}$$

The average of the eigensum in (5) can be determined as [31]

$$E\{D_f\} = D_{f0} = \left(\frac{\pi R_1 R_2}{\lambda L}\right)^2, \tag{7}$$

where $D_{f0}$ is the number of DoFs of the turbulence-free FSO channel (in the near field) or more precisely the eigensum of SVD of the vacuum-propagation Green's function, $h_0(\mathbf{r}, \mathbf{r}')$, which can be obtained by removing the term $e^{\chi(\mathbf{r},\mathbf{r}')+j\varphi(\mathbf{r},\mathbf{r}')}$ from the Green's function in (3). Note that $E\{D_f\} = D_{f0}$ is conveniently expressed as a function of the system geometry, which is, in fact, the product of Fresnel numbers at transmit and receiver apertures.

Figure 3 shows the distribution of the number of DoFs of a FSO channel with $L = 1$ km, $\lambda = 850$ nm and $R_1 = R_2 = 5$ cm over two different turbulence strengths. To generate the samples of the 2D×2D channel $h(\mathbf{r}, \mathbf{r}')$ here and throughout the paper, we use the random phase screen method for the realization of the turbulence effect and the split-step Fourier method [32] to simulate the propagation of the beams through

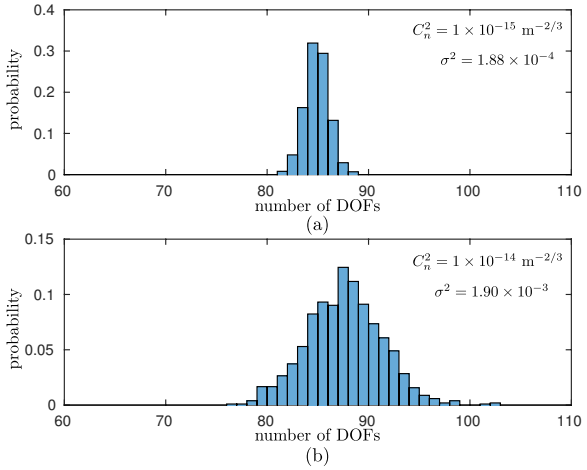


Fig. 3. The histogram of $D_f$ representing the randomness in the available DoFs of the FSO channel with $L = 1$ km, $\lambda = 850$ nm and $R_1 = R_2 = 5$ cm in different turbulence conditions: (a) $C_n^2 = 1 \times 10^{-15}$ m$^{-2/3}$, and (b) $C_n^2 = 1 \times 10^{-14}$ m$^{-2/3}$.

the atmosphere. Moreover, the inner scale and the outer scale of the turbulence are set as $l_0 = 5$ mm and $L_0 = 20$ m, respectively. The phase screens are placed every 50 m which are randomly generated based on the modified von Karman spectrum which is given by

$$\Phi(\kappa) = \beta_1 C_n^2 \left[1 + \beta_2(\kappa/\kappa_l) - \beta_3(\kappa/\kappa_l)^{7/6}\right] \frac{\exp\left(-\kappa^2/\kappa_l^2\right)}{(\kappa_0^2 + \kappa^2)^{11/6}}, \tag{8}$$

where $\beta_1 = 0.033$, $\beta_2 = 1.802$, $\beta_3 = 0.254$, $\kappa_l = 3.3/l_0$, $\kappa_0 = 2\pi/L_0$ and $C_n^2$ is the refractive index structure constant. In Fig. 3, $C_n^2$ that defines the strength of turbulence is assumed as $C_n^2 = 1 \times 10^{-15}$ m$^{-2/3}$ and $C_n^2 = 8 \times 10^{-14}$ which indicate weak and medium turbulence conditions, respectively. We observe that the number of DoFs deviates from the average, (e.g., $D_{f0} \approx 85$ for the FSO system in Fig. 3), over different channel states. It is also observed that the variance of the number of DoFs significantly increases for the stronger turbulence condition.

In the absence of complete CSI and adaptive optics, these number of DoFs cannot be guaranteed since a fixed set of spatial modes needs to be considered for signal transmission while the size of the set should be chosen such that the probability of outage caused by turbulence is significantly reduced. In [33], it is shown that although a fixed mode set cannot adapt to the turbulence channel conditions, achieving large multiplexing gains close to the available number of DoFs would be still possible. However, choosing a fixed set (although orthogonal in the absence of turbulence) would lead to crosstalk among modes as they lose orthogonality under turbulence conditions.

### *B. Spatial Diversity*

So far, we discussed the maximum number of DoFs ($N_{\mathrm{DoF}}$) of FSO systems with a general geometric description developed above. This available number of DoFs implies that in the FSO system in Fig. 2(a), there are $N_{\mathrm{DoF}}$ modes with significant power transfer from the transmitter to the receiver. Therefore, such FSO system can be interpreted as a MIMO system with a size of $N_{\mathrm{DoF}} \times N_{\mathrm{DoF}}$ which provide a maximum multiplexing gain of $M_{\max} = N_{\mathrm{DoF}}$ as in (6). As mentioned earlier, multiplexing gain is not the only advantage of a MIMO system. Particularly, since the FSO channel is a slow fading channel, it is also important to take advantage of the diversity gains of the inherent MIMO structure to enhance its reliability and avoid experiencing long outages induced by turbulence.

In a MIMO FSO diversity systems, CSI is not typically available at the transmitter and a fixed set of input spatial modes needs to be selected through which the copies of the signal are transmitted. In this context, the number of DoFs of the channel only describes the potential power transfer gain of the channel rather than multiplexing gain (as the same signal is transmitted through different modes) or diversity gain (since eigenfunctions are rather spatially orthogonal than statistically independent). In order to get some insights into the spatial diversity gain of the FSO system in Fig. 2(a), we may perform the Karhunen-Loève (KL) decomposition of the distorted optical beam after propagation through the turbulent atmosphere and identify the number of significant eigenvalues in the expansion set [34]. However, the eigenvalues can be only considered as uncorrelated rather than statistically independent as the the distorted beam cannot simply assumed as a Gaussian process. Moreover, the solution of KL expansion of the turbulence-distorted beam is not available for a general input beam distribution although approximations or asymptotic results have been investigated [34].

Here, we therefore present an estimate of the number of statistically independent turbulence modes that can be detected by a receive aperture, which gives an estimation of the receive diversity gain of the FSO link. Consider a sparse receive aperture with infinitesimal subapertues separated by the coherence length of log-amplitude distortion denoted as $l_\chi$. Noting that the log-amplitude fluctuations $\chi$ is modelled as a Gaussian process, the received signals at different subapertures would experience uncorrelated and thus statistically independent log-amplitude fluctuations. The optimal combining (or even equal combing) of the outputs of the subapertures results in a relative diversity gain equal to the number of such subapertures that can be fitted within the constrained aperture area. Therefore, approximating the number of such subapertures by dividing the receive aperture area by the log-amplitude coherence area, the relative receive diversity gain of a direct-detecton FSO system in Fig. 2(a) with respect to a small receive aperture (i.e., $\pi R_2^2 \ll l_\chi^2$) can be estimated as

$$D_r \approx \frac{\pi R_2^2}{l_\chi^2}, \tag{9}$$

which is accurate for large receive apertures, i.e., $\pi R_2^2 \gg l_\chi^2$. The relative diversity gain in (9) can be also confirmed by the literature on aperture averaging receivers [35], [36] where the notion of relative diversity gain can be related to the inverse of aperture averaging factor. Turning from the highly sparse design of the above diversity system towards a near-field monolithic design, a trade-off between the power gain promised by the large $N_{\mathrm{DoF}}$ and the achievable diversity gain

provided by the essentially correlated diversity paths defined by the employed fixed mode set is established. Exploiting this trade-off to achieve the highest reliability at different channel conditions can be the subject of future research.

Considering the reciprocity of the optical atmospheric channel, the diversity gain in (9) also describes the achievable transmit diversity gain of the reverse link, $D'_t = D_r$ as a function of the coherence length of the direct link, $l_\chi$. Note that the log-amplitude coherence length of the reverse link denoted by $l'_\chi$ must be separately measured at the $\mathcal{R}$ plane for beams emitted from the $\mathcal{R}'$ plane and can be different from $l_\chi$. In fact, in space-ground FSO links, the effects of turbulence is not identical in the uplink and downlink (i.e., $l'_\chi \neq l_\chi$) as the atmosphere mostly concentrated closer to the earth while $l'_\chi = l_\chi$ in typical terrestrial FSO links with horizontal atmospheric paths. In effect, the relative transmit diversity gain of the general FSO link in Fig. 2(a) can be similarly written as

$$D_t \approx \frac{\pi R_1^2}{{l'_\chi}^2}. \tag{10}$$

Therefore, using (1), the outage probability $P_{\text{out}}$ of the FSO link decays as

$$P_{\text{out}} \approx e^{-D_t D_r D_S \log(SNR)}, \tag{11}$$

at high SNR where $D_S$ can be defined here as the absolute diversity gain of a FSO system with a single diversity path defined by $\pi R_2^2 \ll l_\chi^2$ and $\pi R_1^2 \ll {l'_\chi}^2$.

Note that this result shows that even for a FSO system in far field (i.e., $D_f < 1$) which only provides a single DoF for communication, it is possible to achieve diversity gain if either transmit or receive aperture is larger than the corresponding log-amplitude coherence area. This is not surprising as conventional $N_t \times 1$ or $1 \times N_r$ MIMO systems can also provide diversity gains of $N_t$ and $N_r$ respectively while they have the same multiplexing gain as a SISO system. Such asymmetrical far-field FSO channels are in fact realized in space-ground applications where the coherence area is much larger than a practical aperture size at the space end while it can be several times smaller than the aperture size at the earth. Therefore, in the uplink space-ground FSO communication, only transmit diversity gain of $D_t$ (with $l'_\chi \approx 10$ cm for near-zenith paths) is possible while only receive diversity gain of $D_r$ (with $l_\chi \approx 10$ cm) can be achieved in the downlink [35].

For most practical terrestrial links (with horizontal paths) affected by weak to intermediate turbulence conditions, we can estimate the log-amplitude coherence length as $l_\chi = l'_\chi \approx \sqrt{\lambda L}$ [37]. Therefore, using equations (9) and (10), the total diversity gain can be written as

$$D = D_t D_r \approx \left(\frac{\pi R_1 R_2}{\lambda L}\right)^2 = D_{f0}, \tag{12}$$

which means that terrestrial FSO systems cannot achieve a relative diversity gain of above unity at far field (i.e., $D_{f0} < 1$ when the total transceiver area is considered) while they may provide a potentially large total relative diversity gain at near field (i.e., $D_{f0} \gg 1$). However, note that this diversity gain is significantly lower than the expected maximum diversity gain from a $D_f \times D_f$ MIMO link (i.e., $D = D_f^2$) which describes the structure of an optimal multiplexing FSO system in near field as discussed above. This diversity gain reduction can be interpreted as the effect of significant correlation among transmit/receive spatial modes in such multi-mode transmission systems.

Moreover, we emphasize that care needs to be taken when analyzing strong turbulence conditions when the shape of coherence area is elongated. In effect, a leveling effect is observed in aperture averaging factor in such strong turbulence conditions for $r_0/2 < R < \lambda L/2r_0$ where $r_0$ is the Fried parameter [12]. However, we can still define the relative diversity gain of a sufficiently large aperture with respect to an aperture with diameter $\lambda L/r_0$ based on the ratio of the aperture areas.

## IV. Performance Analysis of MIMO FSO systems

In this section we evaluate and compare the multiplexing and diversity performance of MIMO FSO systems whether implemented based on monolithic or sparse apertures. We focus on the analysis of practical MIMO FSO systems with direct detection assuming that the full CSI at transmitter or adaptive optics are not available. This is because the use of coherent detection and/or adaptive optics in FSO communications has been so far mostly limited to lab experiments or complex FSO systems developed for space applications. Moreover, the complexity of full CSI acquisition of the $2D \times 2D$ FSO channel quadratically increases by the number of DoFs which could be prohibitive in some practical scenarios where the geometry of the FSO link lies well in the near field regime. In direct detection systems, this issue is even more important as the estimation of phase information would not be straightforward [38]. Note that in the presence of full CSI at the transmitter side, beamforming techniques can be employed to eliminate the interchannel interference and to improve the capacity of the MIMO system based on optimal power allocation [38].

Furthermore, we consider weak and intermediate turbulence conditions in the performance analysis of multiplexing MIMO FSO systems where we show that efficient multiplexing would be possible even without electrical MIMO processing for crosstalk cancellation. On the other hand, we assume a strong turbulence condition when evaluating diversity gain of MIMO FSO systems to emphasize on the importance of spatial diversity in maintaining reliability of the FSO links in such atmospheric condition.

### A. MIMO FSO System Model

The performance analysis of the MIMO FSO system is developed based on the link geometries presented in Figs. 2(a) and 2(b) for monolithic and sparse MIMO, respectively, where limited circular transceiver areas are assumed with radius $R_1 = R_2 = R$. For a fair comparison, we assume that the same number of subapertures and spatial modes are respectively employed in sparse and monolithic MIMO systems. For the sparse MIMO system, the optimal beam waist of the fundamental Gaussian beam that results in minimum received beam waist is employed at the transmitter.

This transmit beam waist can enhance the power gain while reducing the crosstalk introduced by the diffraction effect and hence improve the multiplexing performance [21], [30], [39]. In order to determine this beam waist, consider the relationship between the beamwidth at the receiver plane $w_L$ and that at the transmit plane $w_0$ given by

$$w_L = w_0\sqrt{1+\left(\frac{\lambda L}{\pi w_0^2}\right)^2}. \tag{13}$$

The beam waist at the transmitter $w_0^*$ which minimizes $w_L$ can be expressed as

$$w_0^* = \sqrt{\frac{\lambda L}{\pi}}. \tag{14}$$

Note that $w_0^*$ is a function of wavelength $\lambda$ and the propagating distance $L$. With this optimal beam waist, the beamwidth at the receiver is $w_L^* = \sqrt{\frac{2\lambda L}{\pi}}$. In order to further mitigate the crosstalk among channels induced by diffraction, the sparse subapertures are placed as separated as possible as shown in Fig. 2(b) for three-aperture scenario. At the receiver, the identical design as the transmitter is employed so that each transmitted subaperture is aligned to the corresponding receive subaperture.

For the monolithic MIMO system, the range of spatial mode states that can be fitted within the transmitter area has to be determined. In this paper, we only consider OAM spatial mode set considering that it has attracted significant interest from scientific community recently. However, we would like to emphasize that the analytical derivations and simulations in this paper can also be applied to FSO systems employing other spatial mode sets such as Laguerre-Gaussian (LG) and Hermite-Gaussian (HG) modes. For OAM mode state $l$ the beam waist size is given by [20], [40]

$$w_l = w_0^*\sqrt{|l|+1}, \tag{15}$$

where the transmit beam waist $w_0^*$ is employed for zero mode transmission. The maximal mode state that can fit into the transmit area can be expressed as

$$l_{\max} = \left\lfloor \left(\frac{R}{w_0^*}\right)^2 - 1 \right\rfloor. \tag{16}$$

Equation (16) reveals that $l_{\max}$ is not only associated with the radius $R$ but also with the beam waist for the fundamental Gaussian beam $w_0^*$. Note that Substituting $w_0^*$ and $R$ into (16), one can get the range of OAM modes that can fit into the transceiver area, i.e., $[-l_{\max}, +l_{\max}]$. Even though one can employ all the spatial mode states within $[-l_{\max}, +l_{\max}]$, a multiplexing system becomes crosstalk-limited at high SNR and therefore it is beneficial to limit the number of multiplexing modes. It is shown that for a specific number of transmit modes, in low SNR regime where the system is noise-limited, the mode set with states close to zero mode is preferable due to the better capability of keeping the transmitted power in the intended modes. However, in high SNR regime where the system turns to be crosstalk-limited, the mode set with more separated mode states is preferable due to the minimized inter-mode crosstalk [21]. Similarly, for spatial diversity FSO systems whether implemented by sparse or monolithic apertures, the number of transmit modes or subapertures needs to be limited in order to reduce correlation among diversity paths.

In this work, we consider that three subapertures (or spatial modes) are employed in the sparse (or monolithic) MIMO system. The link distance is chosen as $L = 1$ km and the transmitted beam wavelength is $\lambda = 850$ nm. According to (14), the beam waist of the Gaussian beams at the transmitter plane is $w_0^* = 1.6$ cm. For the sparse MIMO system with three subapertures as shown in Fig. 2(b), the separation between subapertures, $d$, can be expressed as

$$d = \sqrt{3}\,(R - w_0^*)\,, \tag{17}$$

where $d$ should be larger than $2w_0^*$ so that three transmit subapertures can be fitted into the total aperture area. This means that $R \geq \left(\frac{2}{\sqrt{3}}+1\right)w_0^*$. Noting $w_0^* = 1.6$ cm, the minimum total aperture area that can fit at least three subapertures with optimal beam waist transmission is described by the radius $R_{\min} = 3.44$ cm. In our numerical results, we consider total aperture areas with $R = R_{\min}$, as well as with a larger radius $R = R_{\max} = 5$ cm. Without loss of generality, we can assume that the transmit area is centred at the origin so that the coordinates of the three subapertures are given by $(0, R-w_0^*)$, $(-\frac{d}{2}, -\frac{R-w_0^*}{2})$ and $(\frac{d}{2}, -\frac{R-w_0^*}{2})$. In terms of the monolithic MIMO system, the maximal mode state is given by (16). For $R = R_{\min}$ and $R = R_{\max}$, the corresponding range of the mode states is $[-3, +3]$ and $[-8, +8]$, respectively. However, note that the size of these sets are smaller than the average number of available DoFs for such channels which can be calculated based on (7) as $N_{\mathrm{DoF}} \approx 85$ and $N_{\mathrm{DoF}} \approx 19$ for $R = 5$ cm and $R = 3.44$ cm, respectively. This is because we only focussed here on OAM modes that constitute only a part of the LG mode set. Some bounds and estimates for the size of the full LG mode set that can be confined within the transmit and receive aperture areas with radius $R$ are provided in [20] which are consistent with the results presented in the last section.

### *B. Performance of FSO Multiplexing Systems*

Assuming IMDD FSO systems and incoherent superposition of the received signals as modeled in [21], the channel transformation in a FSO multiplexing system with $N_r = N_t = N$ transmit/receive subapertures or modes can be written as

$$\mathbf{y} = \mathbf{H}\mathbf{x} + \mathbf{n}, \tag{18}$$

where $\mathbf{y}$ refers to the vector of the received signal, $\mathbf{x}$ is the vector of transmitted signal, $\mathbf{n}$ is the thermal noise vector and $\mathbf{H}$ is the channel matrix given by

$$\mathbf{H} = \begin{bmatrix} h_{11} & \dots & h_{N1} \\ \vdots & \ddots & \vdots \\ h_{1N} & \dots & h_{NN} \end{bmatrix}, \tag{19}$$

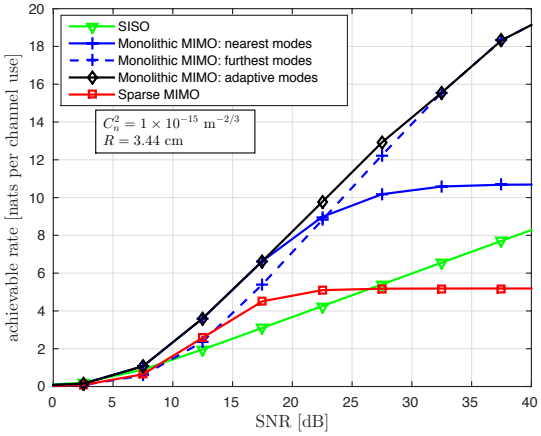


Fig. 4. The average achievable rate for different schemes versus SNR ($P/\sigma$) when $C_n^2 = 1 \times 10^{-15}$ m$^{-2/3}$ and $R = 3.44$ cm. For monolithic system, the nearest modes refer to the mode set $\{-1, 0, +1\}$ and the furthest modes refer to the mode set $\{-3, 0, +3\}$.

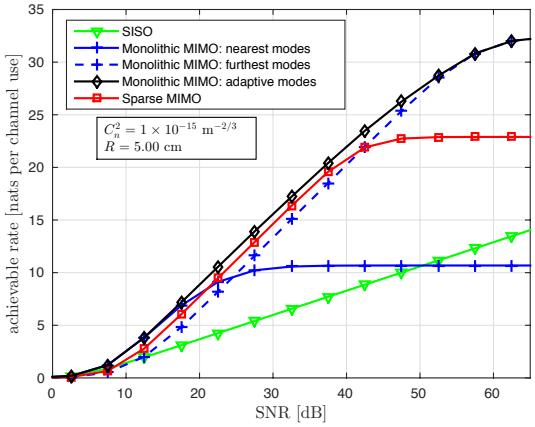


Fig. 5. The average achievable rate for different schemes versus SNR ($P/\sigma$) when $C_n^2 = 1 \times 10^{-15}$ m$^{-2/3}$ and $R = 5$ cm. For monolithic system, the nearest modes refer to the mode set $\{-1, 0, +1\}$ and the furthest modes refer to mode set $\{-8, 0, +8\}$.

where $h_{ij}$ represents the channel gain between the $i$th transmitter and the $j$th receiver. For the $j$th channel, the channel can be expressed as

$$y_j = h_{jj}x_j + \sum_{i \neq j} h_{ij}x_i + n_j. \tag{20}$$

The transmit intensity $x_j$ has to satisfy the average power constraint given by $E[x_j] = P/N$ where we assume that the transmitter has no CSI and allocates the total optical power $P$ uniformly to $N$ channels. In this work, we consider the achievable rates (capacity lower bound) for the multiplexing system. Based on the expression of the capacity lower bound for IM/DD SISO optical channel degraded by the Gaussian noise under an average power constraint given in [41], the achievable rate of the channel given in (20) conditioned on the instantaneous channel matrix $\mathbf{H}$ can be expressed as

$$C_j|_{\mathbf{H}} = \frac{1}{2}\log\left(1 + \frac{e h_{jj}^2 P^2}{2\pi N^2 \sigma_j^2}\right), \tag{21}$$

where the interference plus noise power is given by

$$\sigma_j^2 = \frac{P^2}{N^2}\sum_{i \neq j} h_{ij}^2 + \sigma_n^2. \tag{22}$$

We also assume that the summation of the interference and thermal noise is Gaussian distributed which is an accurate approximation with the increase of the transmitted modes [21]. Denoting the SNR as $\gamma = P/\sigma_n$ [41], (21) can be rewritten as

$$C_j|_{\mathbf{H}} = \frac{1}{2}\log\left[1 + \frac{e h_{jj}^2}{2\pi \sum_{i \neq j} h_{ij}^2 + \frac{2\pi N^2}{\gamma^2}}\right], \tag{23}$$

The average aggregate achievable rate can then be expressed as

$$\bar{C} = E_{\mathbf{H}}\left[\sum_{j=1}^{N} C_j|_{\mathbf{H}}\right]. \tag{24}$$

Figure 4 and Figure 5 show the average achievable rate performances for both sparse and monolithic MIMO systems at a weak turbulence condition ($C_n^2 = 1 \times 10^{-15}$ m$^{-2/3}$) and with $R = 3.44$ cm and $R = 5.00$ cm, respectively. Here, we considered three cases for multiplexing with monolithic MIMO including the transmission of (i) the nearest mode set which can result in the best multiplexing performance in low SNR regime, (ii) the furthest mode set which can result in the best performance in high SNR regime, and (iii) the adaptive mode set which adaptively selects the mode set according to the specific SNR to achieve the highest capacity. Note that the adaptive mode set can be achieved using exhaustive search among all the modes that can be employed in advance for the operating SNR. Note that in the underlying IMDD system, the receive subapertures focus the incident beams to individual detectors in sparse MIMO while this happens after demultiplexer in monolithic MIMO. The performance of a SISO system is also included as a benchmark which is defined as the system with single Gaussian beam transmission with transceiver radius $R = w_0^*$ which is equivalent to $D_f \approx 1$. Note that the transmit power of the SISO scheme is assumed to be equal to the total power of the MIMO FSO scheme and thus it has a power gain with respect to the individual diversity links in the sparse MIMO system.

According to Figs. 4 and 5, one can see that for monolithic MIMO system, the performance of nearest modes is close to that of adaptive modes in low SNR regime and on the other hand the performance of furthest modes is close to adaptive modes in high SNR regime. In addition, the monolithic MIMO systems with nearest and furthest modes outperform the sparse MIMO system in low and high SNR regimes, respectively. In low SNR regime, sparse MIMO performs worse than monolithic MIMO with nearest modes. For instance, when $C_n^2 = 1 \times 10^{-15}$ m$^{-2/3}$ and $R = 3.44$ cm, for sparse MIMO system with $\gamma = 10$ dB the achievable rate is about 1.8 nats per channel use, however, for monolithic MIMO with nearest modes, the corresponding rate is 2.5 nats per channel use. In high SNR regime, sparse MIMO is outperformed

by monolithic MIMO with furthest modes. For instance, For instance, when $C_n^2 = 1 \times 10^{-15}$ m$^{-2/3}$ and $R = 3.44$ cm, for sparse MIMO system with $\gamma = 25$ dB the achievable rate is saturated at 5 nats per channel use, however, for monolithic MIMO with furthest modes, the corresponding rate is 10.4 nats per channel use. Moreover, sparse MIMO performs worse than monolithic MIMO with adaptive modes in the whole investigated SNR range. These results make sense considering that in weak turbulence the degradation of orthogonality between spatial modes induced by turbulence is insignificant and the system is mainly impaired by the power loss due to the limited receiver size. However, for sparse MIMO system, besides the power loss due to limited receiver size, the system further suffers from the crosstalk introduced by the diffraction effects especially when $R$ is small.

When larger transceiver area is considered, higher achievable rate are observed for all of the systems especially for the sparse MIMO and monolithic MIMO with furthest modes. For instance, for $R = 3.44$ cm the achievable rate for sparse system saturates at 5 nats per channel use with the increase of SNR, however, for $R = 5$ cm, the saturate rate increases to 23 nats per channel use. Hence the enhancement is about 4.6 times. This rate increase is due to the decrease of crosstalk between channels with the increase of the distance between subapertures. On the other hand, for monolithic MIMO with furthest modes, the corresponding achievable rate increases from 21 nats per channel use to 32.5 which is about 1.54 times. This improvement is instead caused by the larger separation between transmitted spatial mode states which results in less crosstalk between channels. Compared with SISO system, MIMO systems generally benefit from higher multiplexing gain while relative gains of close to the maximum value of three (as only three DoFs are used) is observed for the monolithic MIMO case at high SNR. With the increase of SNR, however, MIMO systems turn to be crosstalk-limited and the achievable rates gradually saturate at a specific value. However, there in no saturated achievable rate for the SISO system due to the absence of crosstalk from neighbour channels.

We also considered the multiplexing performance of MIMO FSO systems under an intermediate turbulence condition of $C_n^2 = 1 \times 10^{-14}$ m$^{-2/3}$ with $R = 3.44$ cm and $R = 5.00$ cm as presented in Fig. 6 and Fig. 7, respectively, where the achievable rates are significantly degraded compared to the cases under weaker turbulence. For example, with $R = 5.00$ cm, the saturation values for achievable rates decrease from 23 nats per channel use to 16.7 nats per channel use and from 32 nats per channel use to 19.8 nats per channel use for sparse MIMO and monolithic MIMO with adaptive modes, respectively when the $C_n^2$ changes from $C_n^2 = 1 \times 10^{-15}$ m$^{-2/3}$ (see Fig. 5) to $C_n^2 = 1 \times 10^{-14}$ m$^{-2/3}$ (see Fig. 7). For sparse MIMO system, the intermediate turbulence results in stronger beam spreads which lead to less received power from the intended transmitted subapeture and more received crosstalk power from other subapertures. For monolithic MIMO system, intermediate turbulence further destroys the orthogonality between spatial modes and hence introduces more crosstalk between channels.

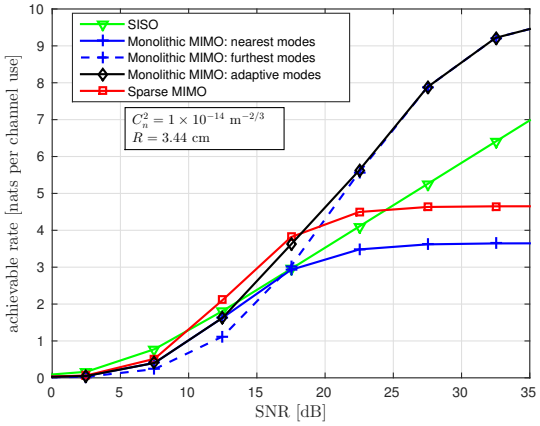


Fig. 6. The average achievable rate for different schemes versus SNR ($P/\sigma$) when $C_n^2 = 1 \times 10^{-14}$ m$^{-2/3}$ and $R = 3.44$ cm. For monolithic system, the nearest modes refer to the mode set $\{-1, 0, +1\}$ and the furthest modes refer to the mode set $\{-3, 0, +3\}$.

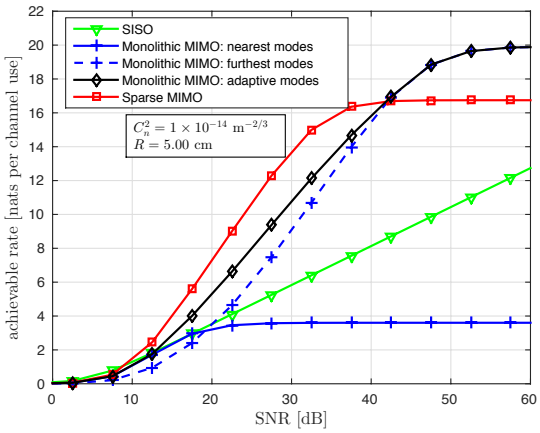


Fig. 7. The average achievable rate for different schemes versus SNR ($P/\sigma$) when $C_n^2 = 1 \times 10^{-14}$ m$^{-2/3}$ and $R = 5$ cm. For monolithic system, the nearest modes refer to the mode set $\{-1, 0, +1\}$ and the furthest modes refer to the mode set $\{-8, 0, +8\}$.

These simulation results also imply that the monolithic MIMO system is degraded more significantly by the turbulence compared to the sparse MIMO system. In addition, by comparing the performance of the sparse and monolithic MIMO systems under intermediate turbulence, one can see that, different from the weak turbulence case, now the sparse MIMO outperforms monolithic MIMO system with adaptive modes in low and moderate SNR regimes. We would like to emphasize that with further stronger turbulence (i.e., $C_n^2 = 1 \times 10^{-13}$ m$^{-2/3}$ which is not shown in this paper), it can be observed that sparse MIMO outperforms monolithic MIMO with adaptive modes in the whole SNR regime.

### C. Performance of FSO Diversity Systems

In this section, we investigate the diversity gain of the underlying sparse and monolithic MIMO systems. At the transmitter side, the copies of the same signal are transmitted using repetition coding [10] either through three subapertures in sparse

MIMO or three spatial modes in monolithic MIMO (referred as spatial mode diversity in [22], [23]). At the receiver side for the monolithic MIMO system, mode demultiplexing process is not considered and a simpler aperture averaging receiver is used. This is because when system is used for mode diversity all the transmitted modes carry the same data and by simply collecting the whole received optical power rather than only the portion of the power remained in the transmitted modes, the system benefits from higher power and diversity gains. For sparse MIMO system, two scenarios are considered for the receiver, (i) a receiver with sparse subapertures, and (ii) an aperture averaging receiver which has a comparable power and receive diversity gains as the monolithic MIMO system. Therefore, for the sparse MIMO, The channel can be expressed as

$$\mathbf{y} = \mathbf{H}\mathbf{x} + \mathbf{n}, \tag{25}$$

where $\mathbf{y}$ refers to the vector of the received signal, $\mathbf{x}$ is the vector of transmitted signal, $\mathbf{n}$ is the thermal noise vector and $\mathbf{H}$ is the channel matrix given by

$$\mathbf{H} = \begin{bmatrix} h_{11} & \dots & h_{N1} \\ \vdots & \ddots & \vdots \\ h_{1N} & \dots & h_{NN} \end{bmatrix}, \tag{26}$$

where $h_{ij}$ represents the channel gain between the $i$th transmit subaperture and the signal detected at $j$th receive subaperture. Considering the repetition coding with $\mathbf{x} = [x, \cdots, x]^T$, the receiver output after EGC combining can be expressed as $Y = \mathbf{1}^T\mathbf{y}$, i.e.,

$$Y = Hx + w, \tag{27}$$

where $H = \sum_{i=1}^{N}\sum_{i=1}^{N} h_{ij}$ and $w$ is the Gaussian noise with variance $\sigma_w^2 = N\sigma_n^2$. When on-off keying (OOK) modulation is employed, $x$ is either 0 or $2P/N$ where $P/N$ is the transmitted optical power per channel. The bit error rate (BER) can be then written as [9]

$$P_e|_H = Q\left(\frac{\sqrt{2}HP}{N\sigma_w}\right). \tag{28}$$

Defining SNR as $\gamma = P/\sigma_n$, (28) can be written as

$$P_e|_H = Q\left(\sqrt{\frac{2H^2\gamma^2}{N^3}}\right). \tag{29}$$

In terms of sparse MIMO with aperture averaging and monolithic MIMO systems, the channel expression can be written as

$$Y' = Hx + n \tag{30}$$

where $H = \sum_{i=1}^{N} g_i$ and $g_i$ is the channel gain between the $i$th transmit subaperture/mode and the receiver. Note that since a single receiver aperture is employed, the introduced thermal noise power is hence $N$ times less than $\sigma_w^2$. Therefore, the conditional bit error probability is given by

$$P_e|_H = Q\left(\sqrt{\frac{2H^2\gamma^2}{N^2}}\right). \tag{31}$$

The average BER can then be expressed as

$$P_e = E_H\left[P_e|_H\right]. \tag{32}$$

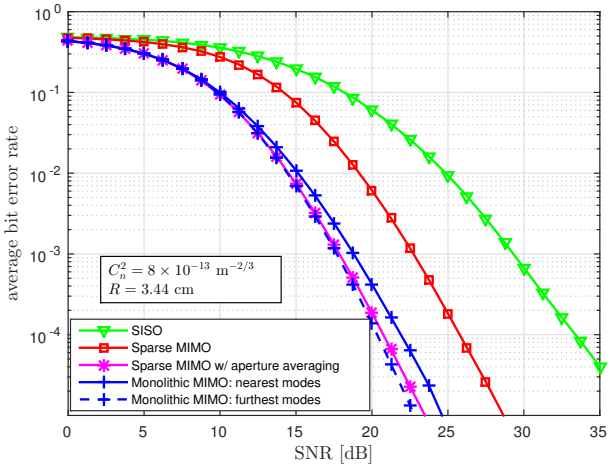


Fig. 8. The average BER versus SNR $\gamma$ when $C_n^2 = 8 \times 10^{-13}$ m$^{-2/3}$ and $R = 3.44$ cm. For monolithic MIMO, the nearest modes refer to the mode set $\{-1, 0, +1\}$ and the furthest modes refer to the mode set $\{-3, 0, +3\}$.

The slope of the average BER curve at high SNR indicates the diversity gain of the system; however, in order to more quantitatively estimate the diversity performance of the underlying systems, we employ the amount of fading (AF) which is defined as the variance-to-mean-square ratio of the channel gain $H$, i.e., $AF = \mathrm{Var}[H]/E[H]$. Therefore, similar to RF communications, the level of AF reduction for MIMO FSO systems with respect to the SISO system should indicate its relative diversity gain.

The average BER with respect to SNR $\gamma$ for sparse and monolithic MIMO systems with transceiver radius $R = 3.44$ cm and $R = 5$ cm is plotted in Fig. 8 and Fig. 9, respectively, under a strong turbulence $C_n^2 = 8\times10^{-13}$ m$^{-2/3}$. Furthermore, the amount of fading of the systems evaluated in Fig. 8 and Fig. 9 are respectively provided in Table I and Table II

It can be observed from Figs. 8 and 9 that compared with SISO, the BER performance can be significantly improved by employing MIMO systems. For instance, for $R = 3.44$ cm, to achieve a BER $P_e = 10^{-4}$ the required SNR is about 33.5 dB, however, in order to achieve the same performance, the required SNR is only 26 dB for sparse MIMO system. If a single large receiver aperture is employed at the receiver, such as sparse MIMO with aperture averaging and monolithic MIMO, the BER performance can be further improved due to the stronger power and diversity gains, and less noise power. For example, the required SNR to achieve $P_e = 10^{-4}$ are 21 dB and 22 dB for sparse MIMO with aperture averaging and monolithic MIMO with nearest modes, respectively. Moreover, it can be seen that the decaying slope of the performance curve is steeper for MIMO systems compared with the SISO systems which represents the realization of diversity gain and these slopes become even steeper for the larger aperture in Fig. 9.

In addition, comparing Fig. 8 and Fig. 9, one can observed that all MIMO systems benefits from larger transceiver systems. For sparse MIMO system, this performance improvement is due to the reduction of fading correlation between

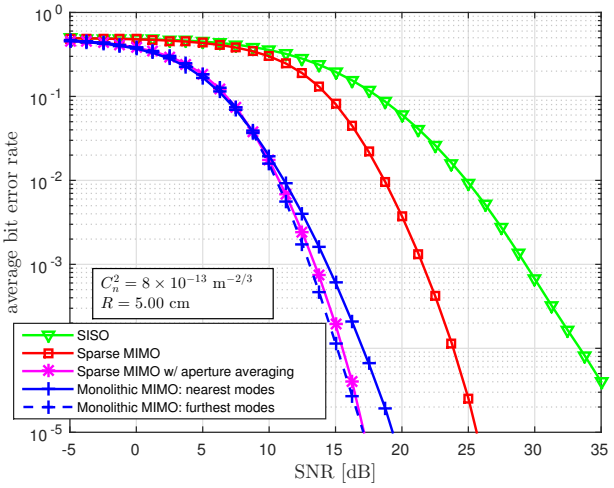


Fig. 9. The average BER versus SNR $\gamma$ when $C_n^2 = 8 \times 10^{-13}$ m$^{-2/3}$ and $R = 5.00$ cm. For monolithic MIMO, the nearest modes refer to the mode set $\{-1, 0, +1\}$ and the furthest modes refer to the mode set $\{-8, 0, +8\}$.

TABLE I
THE AMOUNT OF FADING FOR SYSTEMS IN FIG. 8.

| | Amount of fading |
|---|---|
| SISO | 0.9263 |
| sparse MIMO | 0.2968 |
| sparse MIMO w/ aperture averaging | 0.2528 |
| monolithic MIMO: nearest modes | 0.3155 |
| monolithic MIMO: furthest modes | 0.2417 |

TABLE II
THE AMOUNT OF FADING FOR SYSTEMS FIG. 9.

| | Amount of fading |
|---|---|
| SISO | 0.9263 |
| sparse MIMO | 0.1831 |
| sparse MIMO w/ aperture averaging | 0.1442 |
| monolithic MIMO: nearest modes | 0.1928 |
| monolithic MIMO: furthest modes | 0.1516 |

channels. To see this point more clearly, let's consider the AF results. For $R = 3.44$ cm, the AF of sparse MIMO system is $0.297$ and the AF of SISO system is $0.926$, thus around three times AF reduction can be achieved by employing sparse MIMO (Table I). However, for $R = 5$ cm, the AF for sparse MIMO further reduces to $0.183$ and hence the AF reduction by using sparse MIMO increase to $5$ times (Table II). This is due to the fact that when the transceiver area is large, the apertures at both transmitter and receiver side are more separated which results in less correlation between channels and hence higher AF reduction. Note that in an ideal MIMO system, the AF reduction of using $3 \times 3$ MIMO should be $9$ times compared to SISO system, which is not achieved in our system due to the strong correlation between diversity paths.

For monolithic MIMO system, nearest modes performs worse than furthest modes. For instance, when $R = 5$ cm, $15$ dB SNR is required for the monolithic MIMO system with furthest modes to achieve $P_e = 10^{-4}$, however, if nearest modes are employed, $17$ dB SNR is required. In addition, the AF for monolithic MIMO with nearest modes is $0.193$, but for system with furthest modes the AF reduces to $0.151$. This is because the transmission of separated modes results in less correlation between channels and higher diversity gain as also shown in [22], [23]. Finally, it is interesting to see that the BER performance for monolithic MIMO with furthest modes are similar to that of sparse MIMO with aperture averaging and these two systems also yield similar AF as well. For example, when $R = 5$ cm, the AF for monolithic MIMO with furthest modes is $0.152$ and the AF for sparse MIMO with aperture averaging is $0.144$.

## V. CONCLUSIONS AND FUTURE DIRECTIONS

In this paper, we studied general MIMO FSO systems implemented either with sparse (multiple) or monolithic (single) apertures starting with a general review of the conventional MIMO systems typically designed by multiple apertures. We then presented a unified framework to analyze the diversity and multiplexing gains of such MIMO FSO systems and compare them fairly subject to limited spatial resources of the channel. Our simulation results suggest that both sparse and monolithic MIMO systems can be employed to achieve diversity and similar diversity performance can be achieved. Moreover, multiplexing with monolithic MIMO system is shown to be preferable when turbulence is weak, since the orthogonality between spatial modes is less degraded under weak turbulence, whereas the sparse MIMO suffers from the significant crosstalk introduced by diffraction effects especially when transceiver area is small. With the increase of turbulence condition, however, sparse MIMO system becomes more preferable due to its higher tolerance to the turbulence effects.

MIMO FSO communication is not a new research topic and has already attracted many works in the literature since decades ago; however, the unified framework presented in this paper can open up new research directions on the design of optimal MIMO FSO systems which has been mostly conducted in the literature based on a subset of possible designs, namely, sparse MIMO. In this paper, we only provided basic feasibility results based on some heuristic designs. Therefore, limiting the spatial resources of a FSO link defined by the size of transceivers, it should be possible to design optimal mode transmission and reception techniques for different channel conditions and to achieve different potentials of MIMO systems, including diversity, multiplexing, and power gains. An interesting direction would be to explore the one-to-one trade-offs between diversity, multiplexing, and power gains of MIMO schemes to maximize the capacity and the reliability of the slowly varying FSO channels (e.g., see [23]). Furthermore, it is important to include misalignment errors (which has been ignored in this paper) along with turbulence effects in the optimization analysis as it significantly affects the performance of FSO systems particularly in the near-field regime.

## REFERENCES

[1] H. Dahrouj, A. Douik, F. Rayal, T. Y. Al-Naffouri, and M.-S. Alouini, "Cost-effective hybrid rf/fso backhaul solution for next generation wireless systems," *IEEE Wireless Communications*, vol. 22, no. 5, pp. 98–104, Oct 2015.

[2] S. Rushing, "Analyzing 'global access to the internet for all' projects," *Network Architectures and Services*, vol. 9, pp. 9–15, Jul 2016.

[3] M. Mirhosseini, B. Rodenburg, M. Malik, and R. W. Boyd, "Free-space communication through turbulence: a comparison of plane-wave and orbital-angular-momentum encodings," *Journal of Modern Optics*, vol. 61, no. 1, pp. 43–48, Oct 2014.

[4] S. M. Haas and J. H. Shapiro, "Capacity of wireless optical communications," *IEEE Journal on Selected Areas in Communications*, vol. 21, no. 8, pp. 1346–1357, Oct 2003.

[5] K. Chakraborty, S. Dey, and M. Franceschetti, "Outage capacity of mimo poisson fading channels," *IEEE Transactions on Information Theory*, vol. 54, no. 11, pp. 4887–4907, Nov 2008.

[6] E. J. Lee and V. W. S. Chan, "Part 1: optical communication over the clear turbulent atmospheric channel using diversity," *IEEE Journal on Selected Areas in Communications*, vol. 22, no. 9, pp. 1896–1906, Nov 2004.

[7] M. Razavi and J. H. Shapiro, "Wireless optical communications via diversity reception and optical preamplification," *IEEE Transactions on Wireless Communications*, vol. 4, no. 3, pp. 975–983, May 2005.

[8] S. G. Wilson, M. Brandt-Pearce, Q. Cao, and J. H. Leveque, "Free-space optical MIMO transmission with Q-ary PPM," *IEEE Transactions on Communications*, vol. 53, no. 8, pp. 1402–1412, Aug 2005.

[9] S. M. Navidpour, M. Uysal, and M. Kavehrad, "BER performance of free-space optical transmission with spatial diversity," *IEEE Transactions on Wireless Communications*, vol. 6, no. 8, pp. 2813–2819, Aug 2007.

[10] M. Safari and M. Uysal, "Do we really need ostbcs for free-space optical communication with direct detection?" *IEEE Transactions on Wireless Communications*, vol. 7, no. 11, pp. 4445–4448, Nov 2008.

[11] A. Garcia-Zambrana, C. Castillo-Vazquez, B. Castillo-Vazquez, and A. Hiniesta-Gomez, "Selection transmit diversity for fso links over strong atmospheric turbulence channels," *IEEE Photonics Technology Letters*, vol. 21, no. 14, pp. 1017–1019, Jul 2009.

[12] M.-A. Khalighi, N. Schwartz, N. Aitamer, and S. Bourennane, "Fading reduction by aperture averaging and spatial diversity in optical wireless systems," *J. Opt. Commun. Netw.*, vol. 1, no. 6, pp. 580–593, Nov 2009.

[13] T. A. Tsiftsis, H. G. Sandalidis, G. K. Karagiannidis, and M. Uysal, "Optical wireless links with spatial diversity over strong atmospheric turbulence channels," *IEEE Transactions on Wireless Communications*, vol. 8, no. 2, pp. 951–957, Feb 2009.

[14] E. Bayaki, R. Schober, and R. K. Mallik, "Performance analysis of mimo free-space optical systems in gamma-gamma fading," *IEEE Transactions on Communications*, vol. 57, no. 11, pp. 3415–3424, Nov 2009.

[15] M. Safari and S. Hranilovic, "Diversity and multiplexing for near-field atmospheric optical communication," *IEEE Transactions on Communications*, vol. 61, no. 5, pp. 1988–1997, May 2013.

[16] G. Yang, M. A. Khalighi, S. Bourennane, and Z. Ghassemlooy, "Fading correlation and analytical performance evaluation of the space-diversity free-space optical communications system," *Journal of Optics*, vol. 16, no. 3, pp. 1–10, Mar 2014.

[17] A. E. Willner, G. Xie, L. Li, Y. Ren, Y. Yan, N. Ahmed, Z. Zhao, Z. Wang *et al.*, "Design challenges and guidelines for free-space optical communication links using orbital-angular-momentum multiplexing of multiple beams," *Journal of Optics*, vol. 18, no. 7, pp. 1–13, Jul 2016.

[18] J. Wang, J.-Y. Yang, I. M. Fazal, N. Ahmed, Y. Yan, H. Huang, Y. Ren, Y. Yue, S. Dolinar, M. Tur *et al.*, "Terabit free-space data transmission employing orbital angular momentum multiplexing," *Nature Photonics*, vol. 6, no. 7, pp. 488–496, Jun 2012.

[19] G. Gibson, J. Courtial, M. J. Padgett, M. Vasnetsov, V. Pas'ko, S. M. Barnett, and S. Franke-Arnold, "Free-space information transfer using light beams carrying orbital angular momentum," *Opt. Express*, vol. 12, no. 22, pp. 5448–5456, Nov 2004.

[20] N. Zhao, X. Li, G. Li, and J. M. Kahn, "Capacity limits of spatially multiplexed free-space communication," *Nature Photonics*, vol. 9, no. 12, pp. 822–826, Dec 2015.

[21] J. A. Anguita, M. A. Neifeld, and B. V. Vasic, "Turbulence-induced channel crosstalk in an orbital angular momentum-multiplexed free-space optical link," *Appl. Opt.*, vol. 47, no. 13, pp. 2414–2429, May 2008.

[22] G. R. Mehrpoor, M. Safari, and B. Schmauss, "Free space optical communication with spatial diversity based on orbital angular momentum of light," in *Optical Wireless Communications (IWOW), 2015 4th International Workshop on*. IEEE, Sep 2015, pp. 78–82.

[23] S. Huang, G. R. Mehrpoor, and M. Safari, "Spatial-mode diversity and multiplexing for fso communication with direct detection," *arXiv preprint arXiv:1709.00370*, Sep 2017.

[24] D. L. Fried, "Optical heterodyne detection of an atmospherically distorted signal wave front," *Proceedings of the IEEE*, vol. 55, no. 1, pp. 57–77, Jan 1967.

[25] S. M. Alamouti, "A simple transmit diversity technique for wireless communications," *IEEE Journal on Selected Areas in Communications*, vol. 16, no. 8, pp. 1451–1458, Oct 1998.

[26] M. K. Simon and V. A. Vilnrotter, "Alamouti-type space-time coding for free-space optical communication with direct detection," *IEEE Transactions on Wireless Communications*, vol. 4, no. 1, pp. 35–39, Jan 2005.

[27] N. Letzepis and A. G. I. Fabregas, "Outage probability of the gaussian mimo free-space optical channel with ppm," *IEEE Transactions on Communications*, vol. 57, no. 12, pp. 3682–3690, Dec 2009.

[28] A. A. Farid and S. Hranilovic, "Diversity gain and outage probability for mimo free-space optical links with misalignment," *IEEE Transactions on Communications*, vol. 60, no. 2, pp. 479–487, Feb 2012.

[29] A. García-Zambrana, C. Castillo-Vázquez, and B. Castillo-Vázquez, "Outage performance of mimo fso links over strong turbulence and misalignment fading channels," *Opt. Express*, vol. 19, no. 14, pp. 13 480–13 496, Jul 2011.

[30] J. A. Anguita, M. A. Neifeld, and B. V. Vasic, "Spatial correlation and irradiance statistics in a multiple-beam terrestrial free-space optical communication link," *Appl. Opt.*, vol. 46, no. 26, pp. 6561–6571, Sep 2007.

[31] J. H. Shapiro, "Normal-mode approach to wave propagation in the turbulent atmosphere," *Applied optics*, vol. 13, no. 11, pp. 2614–2619, Nov 1974.

[32] J. D. Schmidt, "Numerical simulation of optical wave propagation with examples in MATLAB." SPIE Bellingham, WA, 2010.

[33] N. Chandrasekaran and J. H. Shapiro, "Photon information efficient communication through atmospheric turbulence–part i: channel model and propagation statistics," *Journal of Lightwave Technology*, vol. 32, no. 6, pp. 1075–1087, Mar 2014.

[34] E. V. Hoversten, R. Harger, and S. Halme, "Communication theory for the turbulent atmosphere," *Proceedings of the IEEE*, vol. 58, no. 10, pp. 1626–1650, Oct 1970.

[35] J. Shapiro, "Imaging and optical communication through atmospheric turbulence," in *Laser Beam Propagation in the Atmosphere*. Springer, Jul 1978, pp. 171–222.

[36] L. C. Andrews, R. L. Phillips, and C. Y. Hopen, *Laser beam scintillation with applications*. SPIE press, 2001, vol. 99.

[37] X. Zhu and J. M. Kahn, "Free-space optical communication through atmospheric turbulence channels," *IEEE Transactions on Communications*, vol. 50, no. 8, pp. 1293–1300, Aug 2002.

[38] S. Huang and M. Safari, "Spatial-mode multiplexing with zero-forcing beamforming in free space optical communications," in *Communications Workshops (ICC Workshops), 2017 IEEE International Conference on*. IEEE, May 2017, pp. 331–336.

[39] G. Xie, L. Li, Y. Ren, H. Huang, Y. Yan, N. Ahmed, Z. Zhao, M. P. J. Lavery, N. Ashrafi, S. Ashrafi, R. Bock, M. Tur, A. F. Molisch, and A. E. Willner, "Performance metrics and design considerations for a free-space optical orbital-angular-momentum-multiplexed communication link," *Optica*, vol. 2, no. 4, pp. 357–365, Apr 2015.

[40] R. L. Phillips and L. C. Andrews, "Spot size and divergence for laguerre gaussian beams of any order," *Appl. Opt.*, vol. 22, no. 5, pp. 643–644, Mar 1983.

[41] A. Lapidoth, S. M. Moser, and M. A. Wigger, "On the capacity of free-space optical intensity channels," *IEEE Transactions on Information Theory*, vol. 55, no. 10, pp. 4449–4461, Oct 2009.